ORIGINAL RESEARCH

Indole and synthetic derivative activate chaperone expression to reduce polyQ aggregation in SCA17 neuronal cell and slice culture models

Pin-Jui Kung[1,*]
Yu-Chen Tao[1,*]
Ho-Chiang Hsu[1]
Wan-Ling Chen[1]
Te-Hsien Lin[1]
Donala Janreddy[2]
Ching-Fa Yao[2]
Kuo-Hsuan Chang[3]
Jung-Yaw Lin[1]
Ming-Tsan Su[1]
Chung-Hsin Wu[1]
Guey-Jen Lee-Chen[1]
Hsiu-Mei Hsieh-Li[1]

[1]Department of Life Science,
[2]Department of Chemistry, National
Taiwan Normal University, Taipei,
Taiwan; [3]Department of Neurology,
Chang Gung Memorial Hospital,
Chang Gung University College
of Medicine, Taipei, Taiwan

*These authors contributed equally
to this work

Correspondence: Guey-Jen Lee-Chen
Department of Life Science, National
Taiwan Normal University, 88 Ting-Chou
Rd, Sec 4, Taipei 11677, Taiwan
Tel +886 2 7734 6359
Fax +886 2 2931 2904
Email t43019@ntnu.edu.tw

Hsiu-Mei Hsieh-Li
Department of Life Science, National
Taiwan Normal University, 88 Ting-Chou
Rd, Sec 4, Taipei 11677, Taiwan
Tel +886 2 7734 6354
Fax +886 2 2931 2904
Email hmhsieh@ntnu.edu.tw

Abstract: In spinocerebellar ataxia type 17 (SCA17), the expansion of a translated CAG repeat in the TATA box binding protein (TBP) gene results in a long polyglutamine (polyQ) tract in the TBP protein, leading to intracellular accumulation of aggregated TBP and cell death. The molecular chaperones act in preventing protein aggregation to ameliorate downstream harmful events. In this study, we used Tet-On SH-SY5Y cells with inducible SCA17 TBP/Q_{79}-green fluorescent protein (GFP) expression to test indole and synthetic derivative NC001-8 for neuroprotection. We found that indole and NC001-8 up-regulated chaperone expression to reduce polyQ aggregation in neuronal differentiated TBP/Q_{79} cells. The effects on promoting neurite outgrowth and on reduction of aggregation on Purkinje cells were also confirmed with cerebellar primary and slice cultures of SCA17 transgenic mice. Our results demonstrate how indole and derivative NC001-8 reduce polyQ aggregation to support their therapeutic potentials in SCA17 treatment.

Keywords: spinocerebellar ataxia type 17, TATA box binding protein, polyQ aggregation, indole and derivative, therapeutics

Introduction

A large number of human disorders are caused by protein misfolding interfering with diverse cellular processes.[1] This is well illustrated by polyglutamine (polyQ)-mediated diseases such as Huntington's disease and some forms of spinocerebellar ataxias (SCA).[2–9] As misfolded polyQ proteins result in aberrant protein aggregate accumulation, the inhibition of aggregation is expected to also inhibit the associated downstream pathogenic events.[10]

Among the polyQ-mediated SCA, SCA type 17 (SCA17) is caused by an expanded polyQ in the TATA-box binding protein (TBP).[9] In humans, the polyQ tract of TBP normally contains 25–42 glutamine residues.[11] TBP repeat expansions of greater than 43 repeats were found not only in the patients with cerebellar degeneration[9,12–14] but also in those with Parkinson's disease, Alzheimer's disease, multiple system atrophy-cerebellar type, and psychiatric disorders.[15–18]

Heat shock proteins (HSPs) are a group of evolutionarily conserved chaperones that possess housekeeping function under physiological conditions to assist in protein folding, transport, and refolding.[19] Under conditions of stress, inducible HSPs are highly up-regulated by heat shock factors (HSFs) to maintain cellular homeostasis and develop cell survival functions.[20,21] HSP70, the most conserved of the HSP families, includes the cytosolic and nuclear constitutive HSC70 (HSPA8, heat shock 70 kDa protein 8) and the stress-inducible HSP70 (HSPA1A, heat shock 70 kDa protein 1A)

proteins.[22] Overexpression of the HSP70 chaperone suppresses neuropathology and improves motor functions in mouse and *Drosophila* models of polyglutamine diseases.[23–25]

Indole is composed of a benzene ring fused to a nitrogen-containing pyrrole ring. Its derivatives are potent anticancer agents widely studied in treating cancers.[26,27] In contrast, their potential in neurodegenerative diseases has not been well known. In this study, we found the antiaggregation effect of indole and synthetic derivative NC001-8 in SCA17 TBP/Q_{79} cell model by enhancing chaperone expression. This antiaggregation effect was further confirmed by cerebellar primary and slice cultures from SCA17 transgenic mice. Our findings provide evidence that indole and its synthetic derivative NC001-8 may have therapeutic potential in treating polyQ-mediated SCA.

Materials and methods
Cell culture and cell proliferation assay
Human neuroblastoma SH-SY5Y cells (American Type Culture Collection no CRL-2266) were cultivated in Dulbecco's Modified Eagle's Medium F12 medium containing 10% fetal bovine serum at 37°C in an incubator with 5% CO_2 atmosphere. Cell proliferation was measured by using Hoechst-propidium iodide (PI) staining. Briefly, cells (5×10^4) were plated into 48 well dishes, grown for 20 hours, and treated with 100 nM–100 µM geranylgeranylacetone (GGA, a potent HSP inducer; Sigma), indole (Sigma), and synthetic derivative NC001-8.[28] After 24 hours, cells were stained with Hoechst 33342 (0.1 µg/mL, Sigma) and PI (5 µg/mL, Sigma), and images of the cells were automatically obtained using MetaXpress Image Acquisition and Analysis Software (Molecular Devices), with excitation/emission wavelengths at 346/460 (Hoechst) and 535/617 (PI).

Triple fluorescent reporter cells and fluorescent assay
A pcDNA5/FRT/TO-derived fluorescent reporter plasmid with mCherry, ZsYellow1, and AmCyan1 reporters driven by HSF1 (to enhance chaperone expression), heat shock cognate protein (HSPA8, to drive constitutively expressed HSP70), and heat-inducible HSP70 chaperone (HSPA1A, to drive heat-inducible HSP70) promoter fragments, respectively, was cloned as described.[29] The resulting plasmid was used to generate triple fluorescent reporter cells and maintained in accordance with the supplier's instructions (Invitrogen). GGA, indole, or NC001-8 (100 nM~100 µM) was added to the medium for 24 hours. The red (HSF1, mCherry), yellow (HSPA8, ZsYellow1), and cyan (HSPA1A, AmCyan1)

fluorescence colors were analyzed simultaneously at 453/486 (mCherry), 531/540 (ZsYellow1), and 587/610 nm (AmCyan1), using automated microscopy combined with an automated image analysis system (ImageXpressMICRO; Molecular Devices).

TBP cDNA constructs and SH-SY5Y TBP cell lines
The cloning of full-length TBP/$Q_{36~79}$ cDNAs in pGEM-T Easy was as described.[30] The *Eco*RI (in MCS of pGEM-T Easy)-*Rsa*I fragment containing the N terminus of TBP (160 amino acids for TBP/Q_{36}) was removed and cloned into pEGFP-N1. Next, a *Hin*dIII-*Not*I DNA fragment containing in-frame TBP/$Q_{36~79}$-GFP was cloned into the pcDNA5/FRT/TO, and the resulting plasmids were used to establish the Flp-In TBP/$Q_{36~79}$ cells using the SH-SY5Y-derived Flp-In host cell line described previously.[30] The CAG repeats in these TBP cell lines were confirmed by polymerase chain reaction and sequencing.

SH-SY5Y TBP/$Q_{36~79}$ aggregation and outgrowth assays
SH-SY5Y TBP/$Q_{36~79}$-GFP cells were seeded in six-well (2×10^5/well) plates in medium containing all-trans retinoic acid (10 µM; Sigma). The next day, doxycycline (5 µg/mL) was added to induce TBP/$Q_{36~79}$-GFP expression for 7~21 days. After that, cells were stained with Hoechst 33342 (0.1 µg/mL; Sigma), and aggregation percentage was assessed by a high content analysis system at 482 (excitation)/536 (emission) wavelengths. The morphologic differentiation of TBP/$Q_{36~79}$ cells, including processes and branches, was assessed by using Metamorph microscopy automation and image analysis software (Molecular Devices). For testing the aggregation reduction potential of GGA, indole, and NC001-8, cells were pretreated with GGA, indole, or NC001-8 (0.1 µM) for 8 hours before inducing TBP/$Q_{36~79}$-GFP expression for 7 days.

Real-time quantitative PCR
Total RNA from SH-SY5Y TBP lines was extracted using Trizol reagent (Invitrogen). The DNase-treated RNA was quantified and reverse-transcribed to cDNA (SuperScript™ III reverse transcriptase; Invitrogen). The ABI PRISM® 7000 Sequence Detection System (Applied Biosystems) was used to perform real-time quantitative polymerase chain reaction (PCR) experiments. Gene-specific TaqMan fluorogenic probes Hs00920494_ml for TBP and 4326321E for HPRT1 (endogenous control) (Applied Biosystems) and 20 ng cDNA

were added to the amplification reaction. Fold change was calculated using the formula $2^{\Delta Ct}$, $\Delta C_T = C_T$ (control) $-$ C_T (target), in which C_T indicates cycle threshold.

Western blot analysis

Total proteins were prepared using buffer containing 50 mM Tris-HCl at pH 8.0, 150 mM NaCl, 1 mM ethyl-enediaminetetraacetic acid at pH 8.0, 1 mM ethylene glycol tetraacetic acid at pH 8.0, 0.1% sodium dodecyl sulfate, 0.5% sodium deoxycholate, 1% TritonX-100, and protease inhibitor cocktail (Sigma). Proteins (20 µg) were separated by sodium dodecyl sulfate-polyacrylamide gel electrophoresis (10%) and blotted onto nitrocellulose membranes. After blocking, the membrane was probed with HSF1 (1:1,000 dilution; Abnova), HSPA8 (1:500 dilution; Santa Cruz), HSPA1A (1:500 dilution; Santa Cruz), GFP (1:500 dilution; Santa Cruz), or β-actin (1:5,000 dilution; Millipore) at 4°C overnight. Then horseradish peroxidase-conjugated goat antimouse or goat anti-rabbit IgG antibody (1:5,000 dilution; GeneTex) and chemiluminescent substrate (Millipore) were used to detect the immune complexes.

Cerebellar primary culture and immunostaining

The culture protocol was modified from several previous reports.[31–33] Culture medium was based on Neurobasal® medium (Invitrogen) with supplements of 2% B-27 (v/v; Invitrogen), 1 mM adenine (Sigma), 2 mM GlutaMax-I (Invitrogen), 3 mM KCl (Sigma), 5 µg/mL gentamicin (Invitrogen), 100 U/mL penicillin (Invitrogen), and 100 µg/mL streptomycin (Invitrogen). Cerebella were isolated from postnatal day 0~1 (P0–P1) SCA17 mice,[34] cut into small pieces, and incubated with culture medium containing 0.05% trypsin/ethylenediaminetetraacetic acid (Invitrogen) and 20 U/mL DNase I (Sigma) for 15 minutes at 37°C. To stop the proteolytic reaction, medium was replaced with 10% fetal bovine serum and 20 U/mL DNase I. After centrifugation, cells were resuspended in medium with 1% fetal bovine serum. Finally, cells were seeded into 96 well culture plates coated with 100 µg/mL poly-L-lysine (Sigma). All treatments were applied to cells with medium containing 4 µM cytosine arabinoside at day 5 (DIV5). After culture for 18 days, cells were fixed with 4% paraformaldehyde and immunostained with primary antibodies IP3R-1 (for Purkinje cells; 1:1,000 dilution; Santa Cruz) and 1TBP18 (for aggregation; 1:30,000 dilution; QED Bioscience), fluorescence-conjugated secondary antibodies (1:500, Invitrogen), and 4′,6-diamidino-2-phenylindole (DAPI, 1:10,000; Sigma). The staining results

were observed by live-cell image microscope (Leica DMI 4000) and high content analysis (HCA) system.

Organotypic cerebellar slice culture and immunostaining

The cerebellar slice culture protocol was modified from a previous report.[35] Whole brains were isolated from postnatal day 7 SCA17 mice and transferred to ice-cold culture medium containing 50% basal Medium Eagle (Invitrogen), 25% Hank's buffered salt solution (Invitrogen), 25% horse serum (Invitrogen), 0.5% D-glucose (Sigma), 1 mM GlutaMax-I, 100 U/mL penicillin, and 100 µg/mL streptomycin. The cerebellum was separated from the other brain regions in ice-cold medium, and the hemisphere was embedded with low-melting-point agarose (Bio Basic) in D-PBS (Invitrogen). The cerebellum was then cut into 350 µm parasagittal sections with a Vibratome (VT1200S; Leica). To improve the survival rate of cerebellar slices, we continuously bubbled the buffer with 95% O_2 and 5% CO_2 during the sectioning. The slices were then cultured on 0.4 µm pore size culture plate inserts (Millipore) in six-well plates. All treatments were applied to the slices at day 2. After culture for 7 days, cells were immunostained with primary antibodies IP3R-1 and 1TBP18, fluorescence-conjugated secondary antibodies, and 4′,6-diamidino-2-phenylindole, as described earlier. The staining results were observed by confocal microscope.

Statistical analysis

Three independent experiments, each done in triplicate, were performed and values were expressed as the means ± standard deviation. Differences between groups were evaluated by Student's *t*-test or one-way analysis of variance with post hoc Fisher's Least Significant Difference test where appropriate. All *P*-values were two-tailed, with values of $P<0.05$ considered significant.

Results
Indole compounds and cytotoxicity

We have previously shown that novel synthetic indole compound 1,1,3-tri(3-indolyl)cyclohexane inhibits cancer cell growth in lung cancer cells and xenograft models.[36] As an indole compound, indomethacin was reported to induce the expression of HSPs to suppress polyQ aggregation in a cellular model of spinal and bulbar muscular atrophy.[37] Indole and synthetic derivative NC001-8 (Figure 1A) were selected to test their potentials to reduce the polyQ aggregation. GGA, a potent HSP inducer,[38] was included for comparison. Cell viability assays were performed with human neuroblastoma
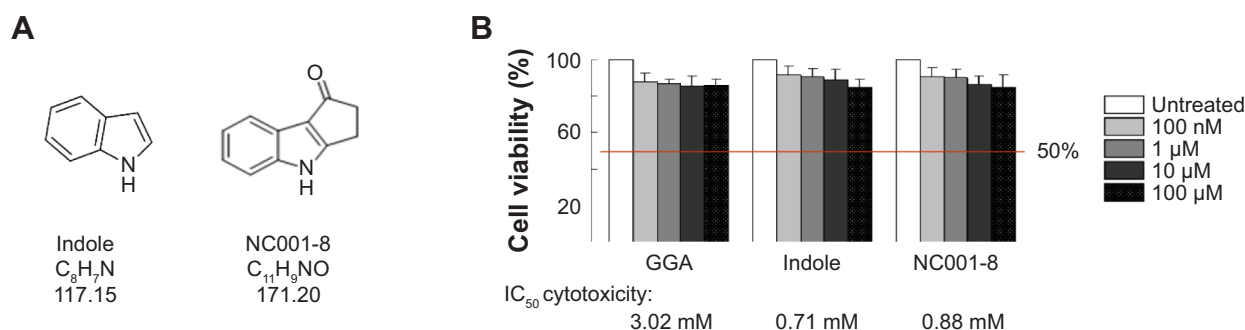
A

Indole
C_8H_7N
117.15

NC001-8
$C_{11}H_9NO$
171.20

B

IC_{50} cytotoxicity:

3.02 mM   0.71 mM   0.88 mM

Figure 1 Indole and derivative NC001-8 and cytotoxicity.
Notes: (**A**) Structure, formula, and molecular weight of indole and synthetic derivative NC001-8. (**B**) Cytotoxicity of GGA, indole, and NC001-8 against SH-SY5Y cells, using Hoechst-propidium iodide staining. Cells were treated with 100 nM~100 μM tested compounds, and cell proliferation was measured the next day (n=3). The half maximal inhibitory concentration of each compound was shown under the columns. To normalize, the relative viability in untreated cells is set as 100%.
Abbreviations: GGA, geranylgeranylacetone; IC_{50}, inhibitory concentration at 50% level.

SH-SY5Y cells after treatment with GGA, indole, or NC001-8 (0.1~100 μM) for 24 hours. The half maximal inhibitory concentrations of the GGA and indoles were calculated using the interpolation method. As shown in Figure 1B, GGA, indole, and NC001-8 had half maximal inhibitory concentrations of 3.02, 0.71, and 0.88 mM, respectively, in SH-SY5Y cells. GGA, indole, and derivative NC001-8 had at least 85% cell viability up to the tested 100 μM, suggesting their low cytotoxicity.

Indole/NC001-8 enhanced HSF1 and HSP70 chaperone expression on HEK-293 cells

To examine the potential of indole/NC001-8 to enhance HSF1 and HSP70 chaperone expression, triple fluorescent reporter cells with mCherry, ZsYellow1, and AmCyan1 reporters driven by HSF1, HSPA8, and HSPA1A promoters were used. As shown in Figure 2A, 1 day GGA treatment (100 nM~100 μM) significantly increases HSF1, HSPA8, and HSPA1A promoter activity (HSF1, 110%~112% [*P*=0.010~0.002]; HSPA8, 106%~116% [*P*=0.024~0.000]; HSPA1A, 108%~118% [*P*=0.034~0.001]). This is also true for 100 nM~100 μM indole treatment, with 117%~125% HSF1 (*P*=0.045~0.030), 118%~125% HSPA8 (*P*=0.046~0.016), and 116%~123% HSPA1A (*P*=0.043~0.011) promoter activities compared with no treatment. For NC001-8 treatment (100 nM~100 μM), HSF1 (111%~123%; *P*=0.042~0.007), HSPA8 (109%~118%; *P*=0.048~0.004), and HSPA1A (106%~121%; *P*=0.042~0.003) promoter activities were also significantly increased. The enhancement of indole and NC001-8 (100 nM) on HSF1 (113%~114%; *P*=0.021~0.007), HSPA8 (108%~109%; *P*=0.046~0.028), and HSPA1A (119%~120%; *P*=0.035~0.001) expression was verified by the Western blot in HEK-293 cells after 2 days of treatment (Figure 2B).

Construction of SH-SY5Y TBP/$Q_{36\sim79}$ lines

To test the aggregation reduction potential of indole and NC001-8 in neuronal cells, we constructed Flp-In SH-SY5Y SCA17 cells with N-terminal TBP/$Q_{36\sim79}$-GFP expression in an inducible fashion. As shown in Figure 3A, real-time polymerase quantification of these TBP lines shows 9~11 times TBP expression after induction with doxycycline for 2 days. In immunoblot, TBP antibody detected 52~62 kDa TBP/$Q_{36\sim79}$-GFP protein in addition to the endogenous 43 kDa TBP protein (Figure 3B). When TBP/$Q_{36\sim79}$ SH-SY5Y cells were differentiated for 7 to 21 days, using retinoic acid,[39,40] a Q length-dependent and expression time-dependent aggregate formation was seen in TBP/$Q_{61\sim79}$-GFP cells, whereas no aggregate was seen in TBP/Q_{36}-GFP cells (Figure 3C). When neuronal phenotype was examined after 7~21 days of differentiation, significantly less process and branch in TBP/Q_{79}-GFP cells was observed at 2~3 weeks of differentiation compared with TBP/Q_{36}-GFP cells (1.63~2.12 versus 1.72~2.38 for process [*P*=0.000~0.002]; 0.37~1.03 versus 0.43~1.31 for branch [*P*=0.043~0.009]) (Figure 3D).

Indole/NC001-8 enhanced HSF1 and HSP70 chaperone expression and reduced TBP/Q_{79} aggregation on SH-SY5Y cell model

The Flp-In SH-SY5Y TBP/Q_{79}-GFP cells discussed earlier were used to examine whether indole and NC001-8 up-regulate HSF1, HSPA8, and HSPA1A expression to reduce aggregation. As shown in Figure 4A, induced expression of TBP/Q_{79} for 6 days attenuated the expression of HSF1 (72%; *P*=0.005), HSPA8 (78%; *P*=0.046), and HSPA1A (84%; *P*=0.047) compared with uninduced
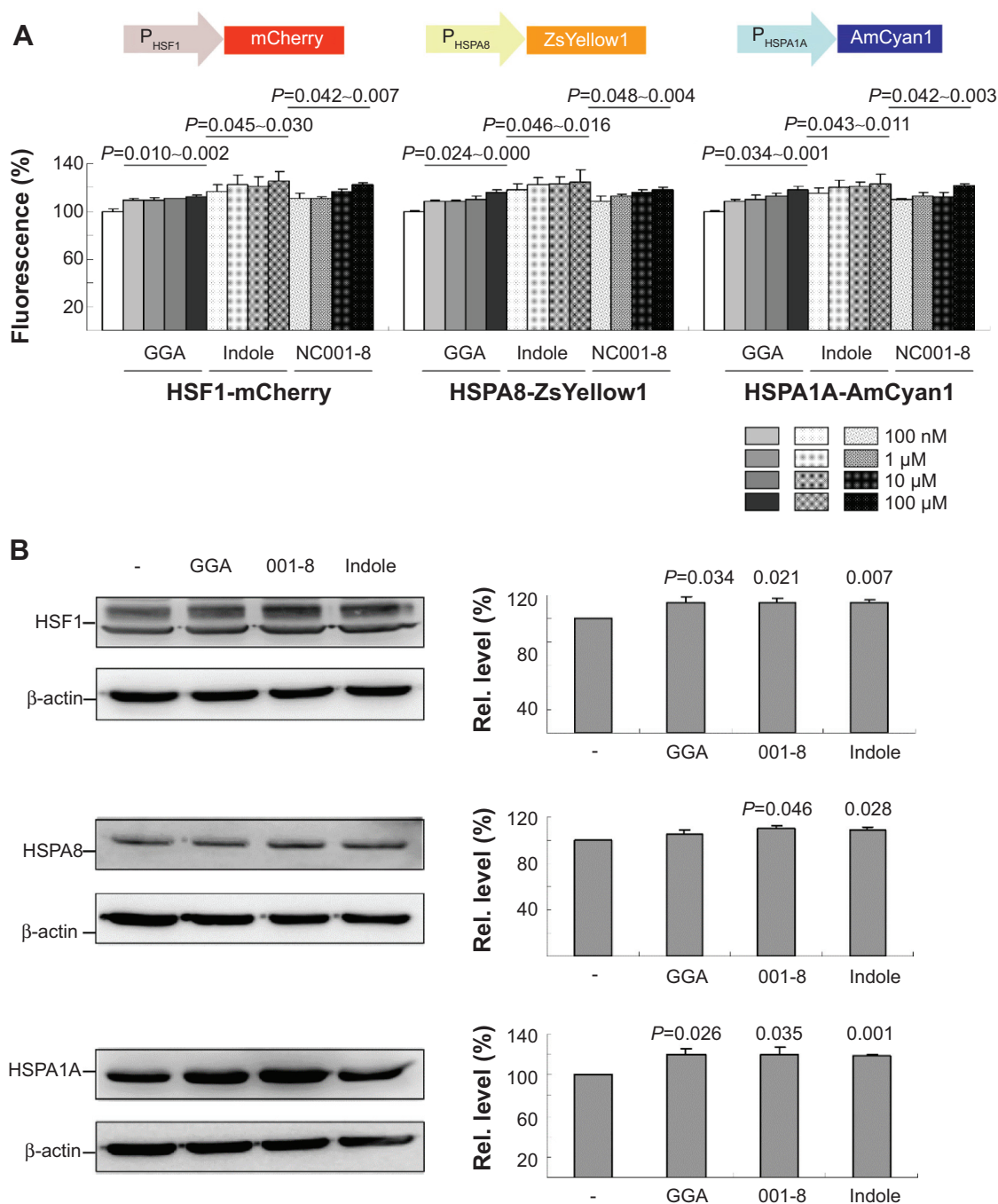
Figure 2 Enhancement of chaperone expression by indole and NC001-8 in HEK-293 cells.
Notes: (**A**) Fluorescent reporters mCherry, ZsYellow1, and AmCyan1 driven by HSF1, HSPA8, and HSPA1A promoter fragments, respectively (top), and effects of GGA, indole, and NC001-8 (100 nM~100 μM) on HSF1, HSPA8, and HSPA1A promoter activities (bottom). To normalize, the fluorescence level in untreated cells is set as 100%. Three independent experiments were performed, with $P<0.05$ considered significant. (**B**) Representative Western blot images of HEK-293 cells treated with GGA, indole and NC001-8 (100 nM) for two days, using HSF1, HSPA8, HSPA1A, and β-actin antibodies. Levels of HSF1, HSPA8, and HSPA1A were normalized with a loading control (β-actin). Data are expressed as the mean ± standard deviation values from three independent experiments.
Abbreviations: GGA, geranylgeranylacetone; 001-8, NC001-8; HSF1, heat shock transcription factor 1; Rel., relative; HSPA8, heat shock 70 kDa protein 8; HSPA1A, heat shock 70 kDa protein 1A.

cells (100%). This reduction can be rescued by the addition of GGA, indole, or NC001-8 (100 nM), with significantly increased HSF1 (96%~111%; $P=0.039~0.004$), HSPA8 (99%~105%; $P=0.024~0.011$), and HSPA1A (106%~117%; $P=0.008~0.001$) expression compared with untreated cells

(72%~84%). The treatment of GGA, indole, and NC001-8 led to 17% ($P=0.001$), 15% ($P=0.002$), and 14% ($P=0.010$), respectively, aggregation reduction in TBP/Q$_{79}$ expressed differentiated neuronal cells (Figure 4B). These findings indicate that indole and NC001-8 up-regulated HSF1 and
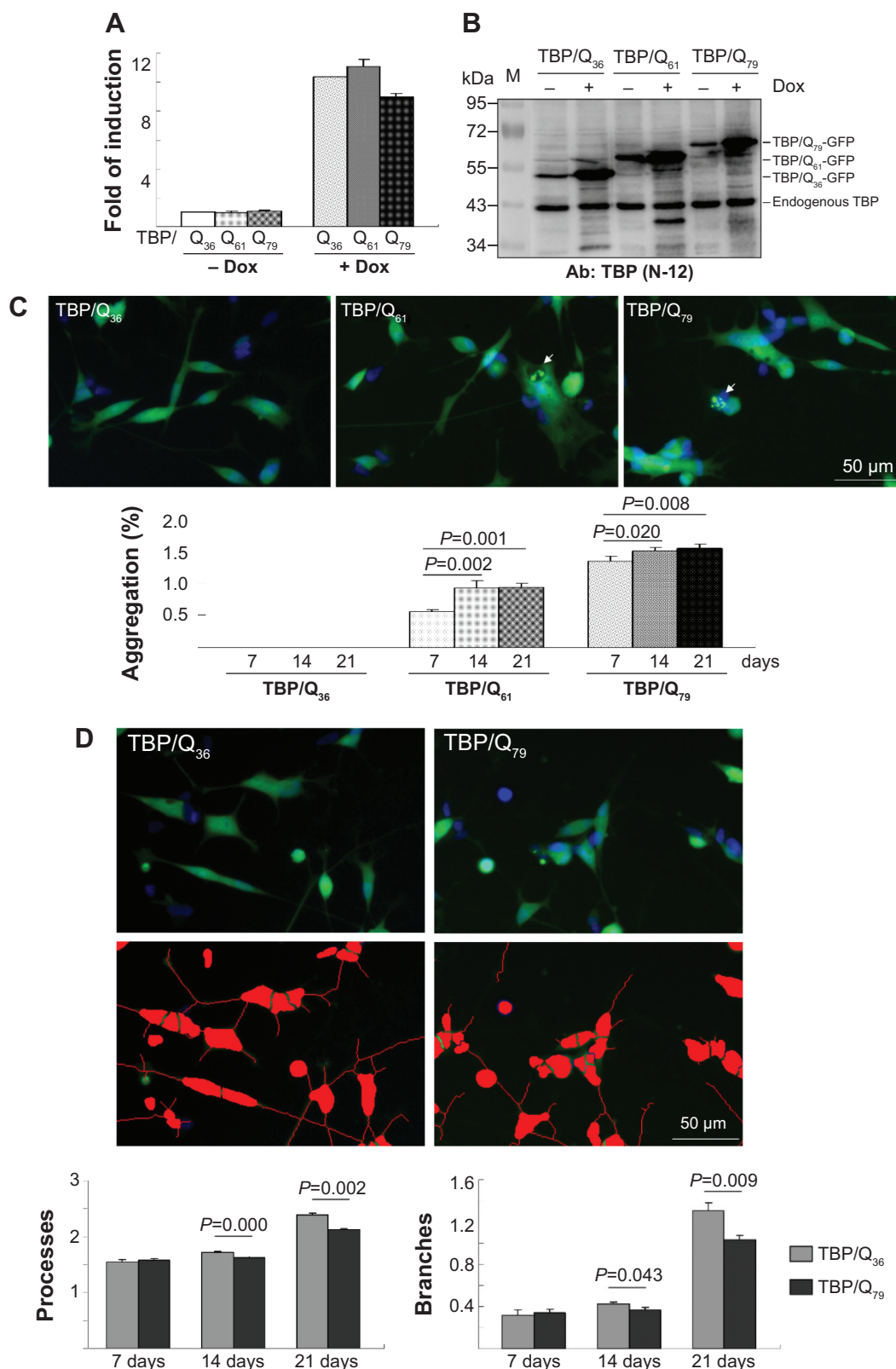
Figure 3 SH-SY5Y cells with induced TBP/Q$_{36-79}$-GFP expression and neuronal phenotype.
Notes: (**A**) Real-time polymerase chain reaction quantification (n=3) of TBP/Q$_{36-79}$-GFP mRNA level relative to HPRT1 mRNA after 2 days of induction with doxycycline (+ Dox) or not (− Dox). (**B**) Western blot analysis of TBP/Q$_{36-79}$-GFP protein level using TBP (N-12) antibody after 2 days of induction with doxycycline (+ Dox) or not (− Dox). (**C**) Representative microscopic images (top) of TBP/Q$_{36-79}$-GFP cells after induced differentiation with retinoic acid (+ RA) for 7 days and aggregate quantification (bottom; n=3) of cells with induced differentiation for 7~21 days. P-values were evaluated by one-way analysis of variance with post hoc LSD test. (**D**) Representative microscopic images (top) of neuronal differentiated TBP/Q$_{36}$ and TBP/Q$_{79}$ cells (for 14 days) and quantification (n=3) of neuronal processes and branches (bottom) of cells with induced differentiation for 7~21 days (blue, nuclei; green, expressed TBP/Q$_{36-79}$-GFP protein; red, cell body and outgrowth segmentation).
Abbreviations: Dox, doxycycline; TBP, TATA box binding protein; GFP, green fluorescent protein; mRNA, messenger RNA; Ab, antibody; LSD, Fisher's least significant difference.
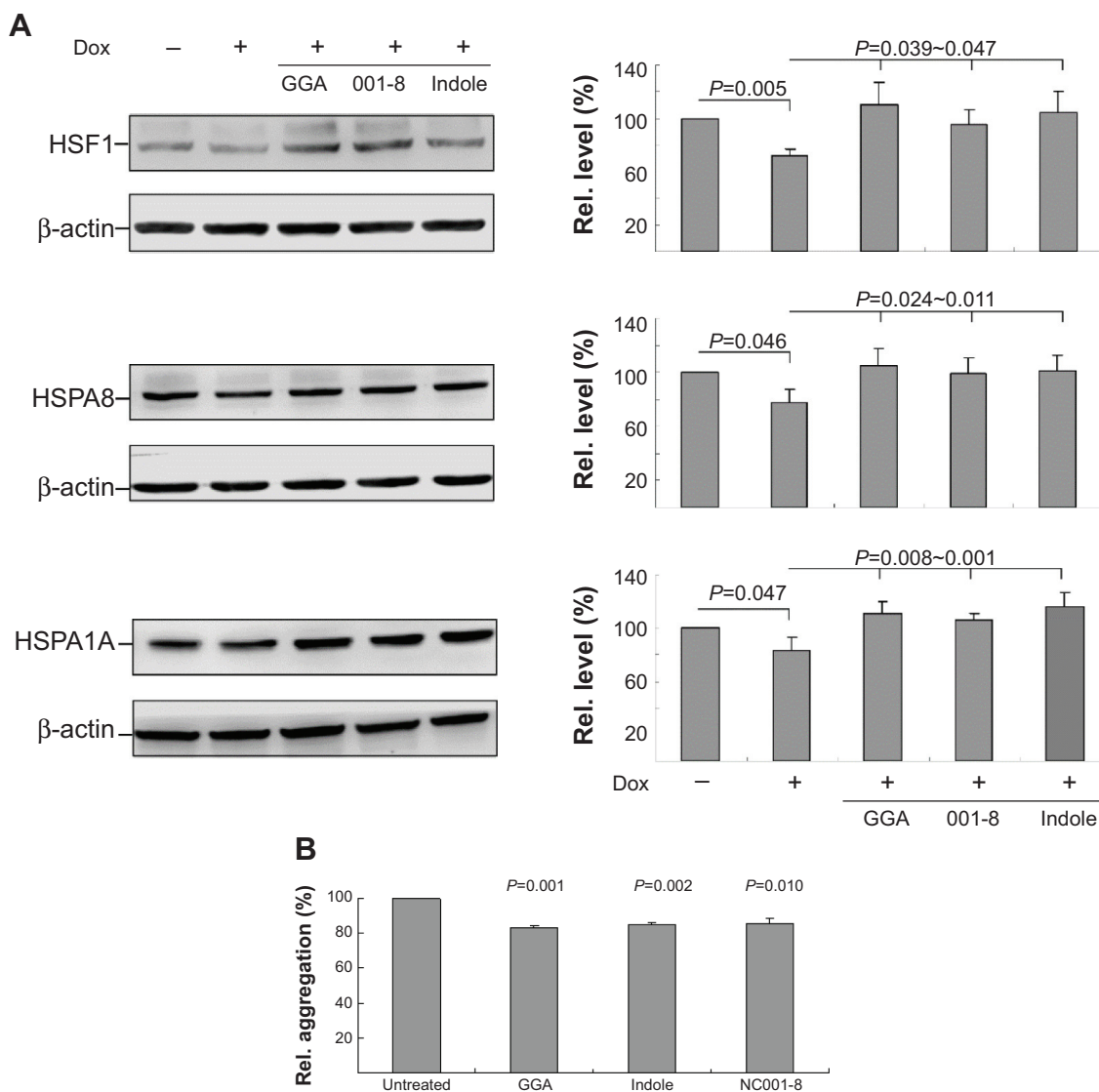
Figure 4 Enhancement of HSF1 and chaperone expression and reduction of aggregation by indole and NC001-8 in neuronal SH-SY5Y TBP/Q_{79} cells.
Notes: (**A**) Cells were pretreated with GGA, indole, or NC001-8 (100 nM) for 8 hours and TBP/Q_{79}-GFP expression induced for 6 days. Relative HSF1, HSPA8, and HSPA1A expressions were analyzed by immunoblot analysis, using β-actin as a loading control (n=3). *P*-values were evaluated by one-way analysis of variance with post hoc LSD test. (**B**) Cells were treated with GGA, indole, or NC001-8 (100 nM) for 7 days, and relative aggregation assessed by HCA system (n=3). To normalize, the relative aggregation level in untreated cells is set as 100%.
Abbreviations: Dox, doxycycline; GGA, geranylgeranylacetone; HSF1, heat shock transcription factor 1; HSPA8, heat shock 70 kDa protein 8; HSPA1A, heat shock 70 kDa protein 1A; Rel., relative; GFP, green fluorescent protein; HCA: high content analysis; 001-8, NC001-8; LSD, Fisher's least significant difference.

HSP70 chaperone expression to reduce TBP/Q_{79} aggregation in differentiated neuronal cell models.

Indole/NC001-8 promoted Purkinje cell neurite outgrowth and reduced aggregation on SCA17 mouse primary and slice cultures

To further confirm the neuroprotective potential of the indole compounds, we applied indole and NC001-8 to the cerebellar primary and slice cultures established from SCA17 mice.[34] As shown in Figure 5A-B, with 10~100 nM compound concentration, significantly (indole: 134%~149%;

P=0.016~0.002) or notably (NC001-8: 114%~119%; P>0.05) increased Purkinje cell neurite outgrowth was observed. Both compounds at concentrations 1~100 nM significantly reduced the Purkinje cell aggregation on the primary culture (indole: P=0.039~0.001; NC001-8: P=0.042~0.016). The percentage of cells with aggregates under indole treatment is 86% (1 nM), 71% (10 nM), and 53% (100 nM) in Figure 5A, and the percentage of cells with aggregates under NC001-8 treatment is 60% (1 nM), 68% (10 nM), and 60% (100 nM) in Figure 5B. On SCA17 mouse cerebellar slice culture, although indole at 10 nM could significantly reduce the Purkinje cell aggregation (28%;
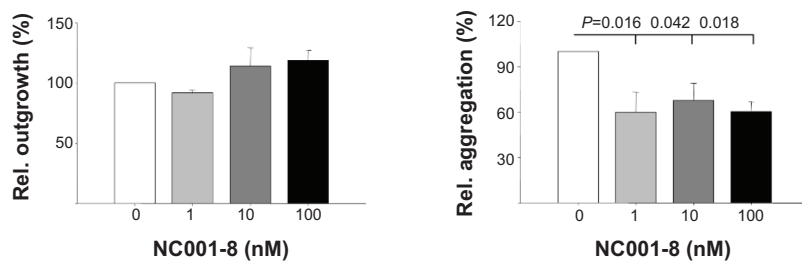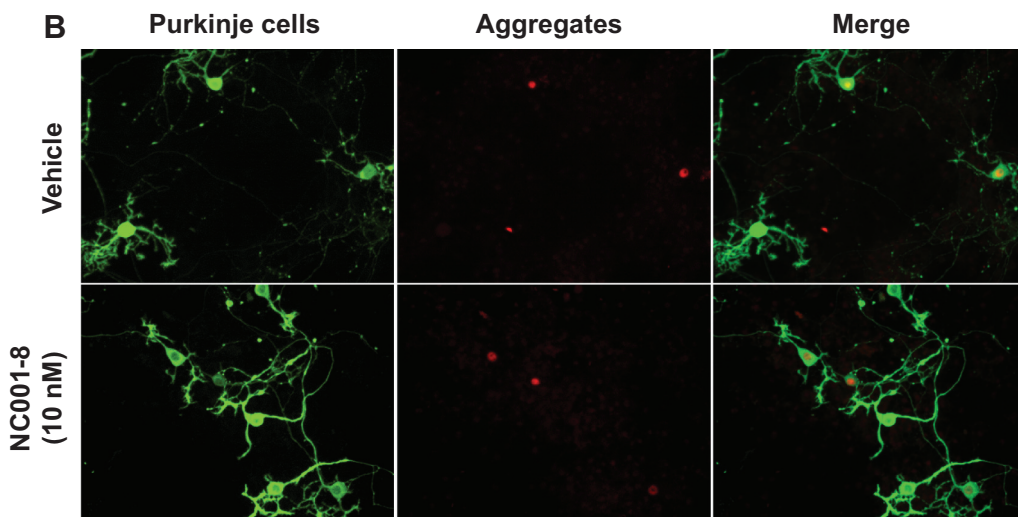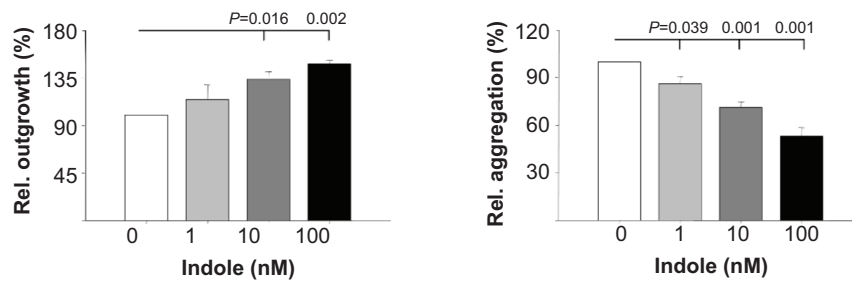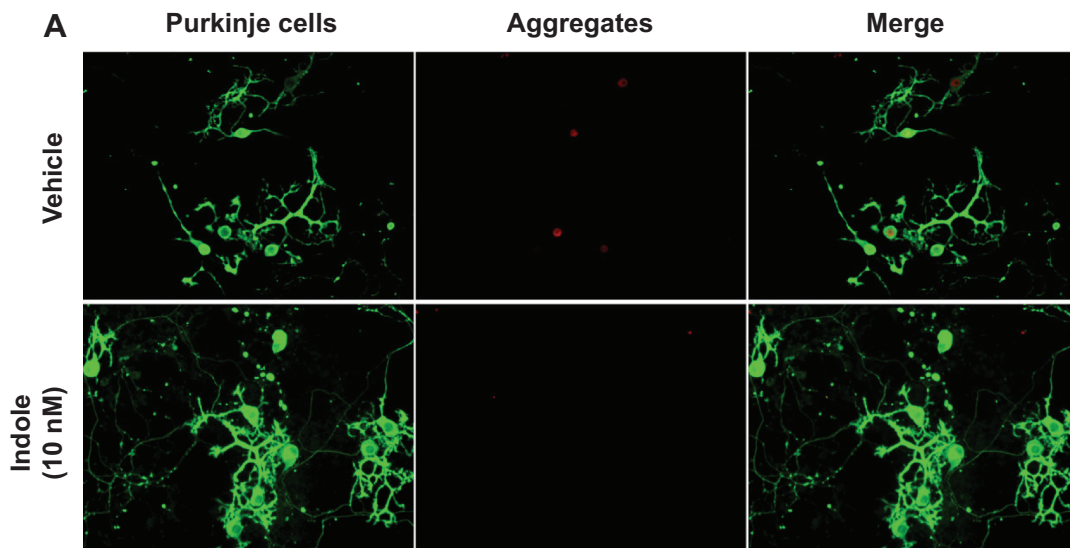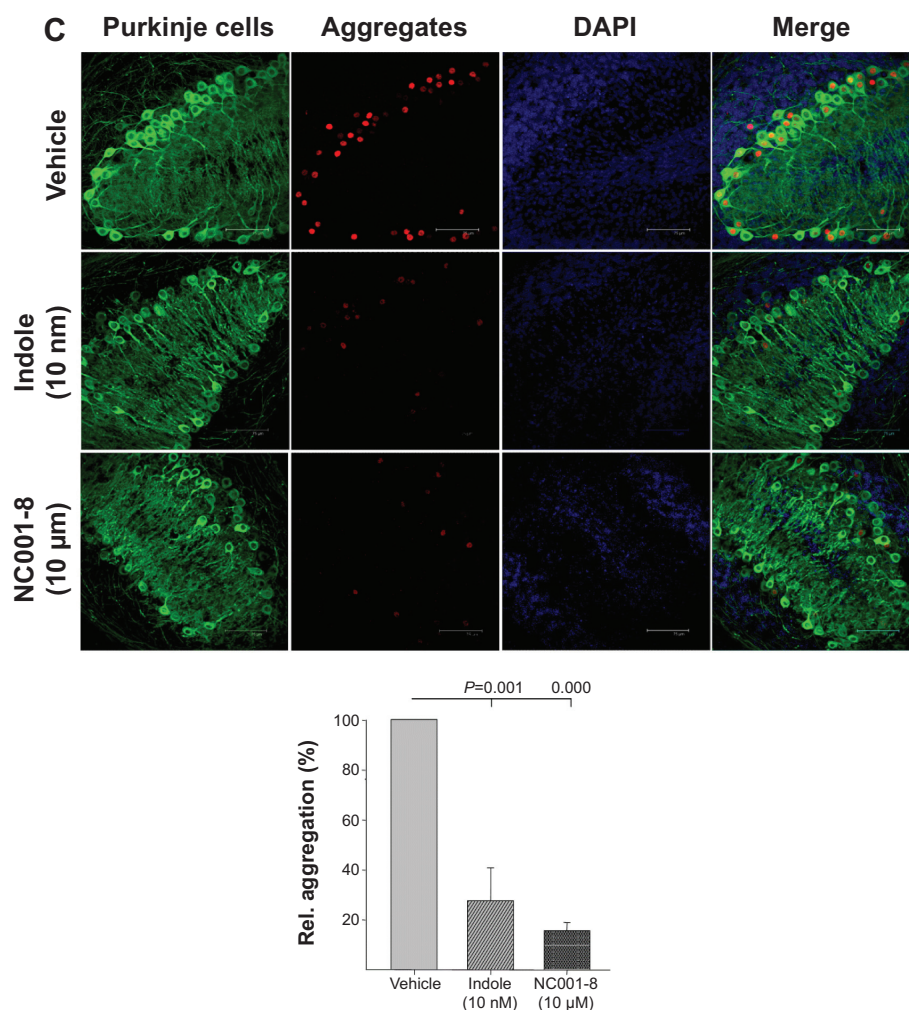
Figure 5 (*Continued*)

Figure 5 Indole and NC001-8 promoted neurite outgrowth and reduced aggregation of Purkinje cells in spinocerebellar ataxia type 17 mouse cerebellar primary and slice cultures.

Notes: The primary culture was treated with 0~100 nM indole (**A**) or NC001-8 (**B**) for 13 days. The representative microscopic images of treatment with 100 nM indole or NC001-8 are shown, and the relative Purkinje cell neurite outgrowth (green) and aggregation (shown in white in the middle column and in red in the right merged column) were quantified (n=3). (**C**) The slice culture was treated with 10 nM indole or 10 μM NC001-8 for 6 days. The representative microscopic images of treatment are shown, and the relative Purkinje cell aggregation (red) was quantified (n=3). To normalize, the relative neurite outgrowth length and aggregation level in vehicle-treated cells or slices is set as 100%. IP3R-1 and 1TBP18 antibodies were used to detect the Purkinje cells and TBP aggregation, respectively.

Abbreviations: IP3R-1, inositol 1,4,5 trisphosphate receptor type 1; 1TBP18, mouse monoclonal antibody to TATA binding protein (TBP); Rel., relative; DAPI, 4′,6-diamidino-2-phenylindole.

$P=0.001$), 1,000 folds of NC001-8 (10 μM) were required to obtain a significant reduction of the aggregation (16%; $P<0.001$) (Figure 5C). Thus, indole worked more efficiently than NC001-8 in reducing the Purkinje cell aggregation on SCA17 mouse cerebellar slice culture.

Discussion

An amount of evidence has indicated indole compounds as efficacious low-molecular drugs for the treatment of cancers. For example, indole-3-carbinol has been shown to suppress the proliferation and induce apoptosis and cell cycle arrest of a wide variety of cancer cells.[41,42] Nevertheless, attempts to apply these chemicals in treating polyQ diseases are still too few. Previously, indole compound indomethacin induced the expression of HSPs at physiological temperatures to suppress the protein aggregation and apoptosis caused by an expansion of the polyQ tract in the androgen receptor.[37] In this study, we revealed that indole and its synthetic derivative NC001-8 reduced TBP aggregates in cell line and mouse cerebellar primary and slice cultures. The intact cellular interaction within the slice culture makes inadequate penetration of the medium into the inner part of the slice; therefore, 1,000 folds of NC001-8 were required to reduce polyQ-induced aggregation in slice culture compared with cell line and primary culture. In addition, our data show that indole and NC001-8 reduced TBP aggregates through the activation of HSF1 to

increase cellular levels of HSP70 chaperone. Together, these data suggest the therapeutic potential of indole and derivative for polyQ-expanded SCA.

In polyQ-mediated SCA, the inclusion of the disease-causing proteins affects molecular chaperone pathways.[43] Previously, we showed the decreased heat shock cognate HSPA8 protein (a constitutive HSP70) expression underlying pathogenesis of SCA17.[44,45] HSP70 has been reported to suppress polyQ-mediated neurodegeneration in *Drosophila*.[23,24] Overexpression of heat-inducible HSP70 chaperone (HSPA1A) rescues the severity of polyQ-mediated degeneration and improves motor function in SCA1 mice.[25] Expression of molecular chaperones is regulated by HSF1, and HSF1-activating compounds have been indicated as therapeutic candidates for polyQ disorders.[46,47] Our results of neuroprotection via enhancement of chaperone system provide a novel mechanism of indole and derivative NC001-8 to decelerate the neurodegenerative process.

Although we have shown that both indole and NC001-8 performed neuroprotection via enhancement of chaperone system, pleiotropic effects of these compounds may exist to lead to the neuroprotective effect. For example, indole-3-carbinol from *Brassica* family vegetables was shown to have anti-inflammatory and antioxidative activities,[48,49] which could also benefit polyQ-mediated diseases.[50,51] Future genome-wide expression studies could explore whether there is any other underlying mechanism of these compounds.

To summarize, we provided strong evidence that indole and NC001-8 could be novel therapeutics for SCA17. As indole is the precursor to many pharmaceuticals, and indole and derivatives can be synthesized by all kinds of methods,[52,53] the development of indole-based compounds offers a promising strategy for the treatment of polyQ diseases. Future investigations of indole, NC001-8, and derivatives in more SCA or other polyQ animal models would strengthen their potential in aggregation reduction and disease amelioration.

Acknowledgments

Disclosure

The authors report no conflicts of interest in this work.

References

1. Gomes CM. Protein misfolding in disease and small molecule therapies. *Curr Top Med Chem*. 2012;12(22):2460–2469.
2. MacDonald M; The Huntington's Disease Collaborative Research Group. A novel gene containing a trinucleotide repeat that is expanded and unstable on Huntington's disease chromosomes. *Cell*. 1993;72(6):971–983.
3. Orr HT, Chung MY, Banfi S, et al. Expansion of an unstable trinucleotide CAG repeat in spinocerebellar ataxia type 1. *Nat Genet*. 1993;4(3):221–226.
4. Pulst SM, Nechiporuk A, Nechiporuk T, et al. Moderate expansion of a normally biallelic trinucleotide repeat in spinocerebellar ataxia type 2. *Nat Genet*. 1996;14(3):269–276.
5. Kawaguchi Y, Okamoto T, Taniwaki M, et al. CAG expansions in a novel gene for Machado-Joseph disease at chromosome 14q32.1. *Nat Genet*. 1994;8(3):221–228.
6. Zhuchenko O, Bailey J, Bonnen P, et al. Autosomal dominant cerebellar ataxia (SCA6) associated with small polyglutamine expansions in the α_{1A}-voltage-dependent calcium channel. *Nat Genet*. 1997;15(1):62–69.
7. David G, Abbas N, Stevanin G, et al. Cloning of the SCA7 gene reveals a highly unstable CAG repeat expansion. *Nat Genet*. 1997;17(1):65–70.
8. Moseley ML, Zu T, Ikeda Y, et al. Bidirectional expression of CUG and CAG expansion transcripts and intranuclear polyglutamine inclusions in spinocerebellar ataxia type 8. *Nat Genet*. 2006;38(7):758–769.
9. Koide R, Kobayashi S, Shimohata T, et al. A neurological disease caused by an expanded CAG trinucleotide repeat in the TATA-binding protein gene: a new polyglutamine disease? *Hum Mol Genet*. 1999;8(11):2047–2053.
10. Denny RA, Gavrin LK, Saiah E. Recent developments in targeting protein misfolding diseases. *Bioorg Med Chem Lett*. 2013;23(7):1935–1944.
11. Gostout B, Liu Q, Sommer SS. "Cryptic" repeating triplets of purines and pyrimidines (cRRY(i)) are frequent and polymorphic: analysis of coding cRRY(i) in the proopiomelanocortin (POMC) and TATA-binding protein (TBP) genes. *Am J Hum Genet*. 1993;52(6):1182–1190.
12. Nakamura K, Jeong SY, Uchihara T, et al. SCA17, a novel autosomal dominant cerebellar ataxia caused by an expanded polyglutamine in TATA-binding protein. *Hum Mol Genet*. 2001;10(14):1441–1448.
13. Fujigasaki H, Martin JJ, De Deyn PP, et al. CAG repeat expansion in the TATA box-binding protein gene causes autosomal dominant cerebellar ataxia. *Brain*. 2001;124(Pt 10):1939–1947.
14. Silveira I, Miranda C, Guimarães L, et al. Trinucleotide repeats in 202 families with ataxia: a small expanded (CAG)n allele at the SCA17 locus. *Arch Neurol*. 2002;59(4):623–629.
15. Wu YR, Lin HY, Chen CM, et al. Genetic testing in spinocerebellar ataxia in Taiwan: expansions of trinucleotide repeats in SCA8 and SCA17 are associated with typical Parkinson's disease. *Clin Genet*. 2004;65(3):209–214.
16. Wu YR, Fung HC, Lee-Chen GJ, et al. Analysis of polyglutamine-coding repeats in the TATA-binding protein in different neurodegenerative diseases. *J Neural Transm*. 2005;112(4):539–546.
17. Chen CM, Lane HY, Wu YR, et al. Expanded trinucleotide repeats in the TBP/SCA17 gene mapped to chromosome 6q27 are associated with schizophrenia. *Schizophr Res*. 2005;78(2–3):131–136.
18. Lin IS, Wu RM, Lee-Chen GJ, Shan DE, Gwinn-Hardy K. The SCA17 phenotype can include features of MSA-C, PSP and cognitive impairment. *Parkinsonism Relat Disord*. 2007;13(4):246–249.
19. Hartl FU, Hayer-Hartl M. Molecular chaperones in the cytosol: from nascent chain to folded protein. *Science*. 2002;295(5561):1852–1858.
20. Welch WJ, Gething M-J, Clarke AR, et al. Heat shock proteins functioning as molecular chaperones: their roles in normal and stressed cells. *Philos Trans R Soc Lond B Biol Sci*. 1993;339(1289):327–333.
21. Jäättelä M. Heat shock proteins as cellular lifeguards. *Ann Med*. 1999;31(4):261–271.
22. Daugaard M, Rohde M, Jäättelä M. The heat shock protein 70 family: Highly homologous proteins with overlapping and distinct functions. *FEBS Lett*. 2007;581(19):3702–3710.

23. Warrick JM, Chan HY, Gray-Board GL, Chai Y, Paulson HL, Bonini NM. Suppression of polyglutamine-mediated neurodegeneration in *Drosophila* by the molecular chaperone HSP70. *Nat Genet*. 1999;23(4): 425–428.

24. Iijima-Ando K, Wu P, Drier EA, Iijima K, Yin JC. cAMP-response element-binding protein and heat-shock protein 70 additively suppress polyglutamine-mediated toxicity in *Drosophila*. *Proc Natl Acad Sci U S A*. 2005;102(29):10261–10266.

25. Cummings CJ, Sun Y, Opal P, et al. Over-expression of inducible HSP70 chaperone suppresses neuropathology and improves motor function in SCA1 mice. *Hum Mol Genet*. 2001;10(14):1511–1518.

26. Ahmad A, Biersack B, Li Y, et al. Targeted regulation of PI3K/Akt/ mTOR/NF-κB signaling by indole compounds and their derivatives: mechanistic details and biological implications for cancer therapy. *Anticancer Agents Med Chem*. 2013;13(7):1002–1013.

27. Biersack B, Schobert R. Indole compounds against breast cancer: recent developments. *Curr Drug Targets*. 2012;13(14):1705–1719.

28. Janreddy D, Kavala V, Bosco JWJ, Kuo CW, Yao CF. An easy access to carbazolones and 2,3-disubstituted indoles. *Eur J Org Chem*. 2011; 12(12):2360–2365.

29. Chang KH, Chen WL, Lee LC, et al. Aqueous Extract of Paeonia lactiflora and Paeoniflorin as Aggregation Reducers Targeting Chaperones in Cell Models of Spinocerebellar Ataxia 3. *Evid Based Complement Alternat Med*. 2013;2013:471659.

30. Lee LC, Chen CM, Wang HC, et al. Role of the CCAAT-binding protein NFY in SCA17 pathogenesis. *PLoS ONE*. 2012;7(4):e35302.

31. Furuya S, Makino A, Hirabayashi Y. An improved method for culturing cerebellar Purkinje cells with differentiated dendrites under a mixed monolayer setting. *Brain Res Brain Res Protoc*. 1998;3(2):192–198.

32. Gimenez-Cassina A, Lim F, Diaz-Nido J. Gene transfer into Purkinje cells using herpesviral amplicon vectors in cerebellar cultures. *Neurochem Int*. 2007;50(1):181–188.

33. Tanaka M, Yanagawa Y, Hirashima N. Transfer of small interfering RNA by single-cell electroporation in cerebellar cell cultures. *J Neurosci Methods*. 2009;178(1):80–86.

34. Chang YC, Lin CY, Hsu CM, et al. Neuroprotective effects of granulocyte-colony stimulating factor in a novel transgenic mouse model of SCA17. *J Neurochem*. 2011;118(2):288–303.

35. Birgbauer E, Rao TS, Webb M. Lysolecithin induces demyelination in vitro in a cerebellar slice culture system. *J Neurosci Res*. 2004;78(2): 157–166.

36. Lee CH, Yao CF, Huang SM, et al. Novel 2-step synthetic indole compound 1,1,3-tri(3-indolyl)cyclohexane inhibits cancer cell growth in lung cancer cells and xenograft models. *Cancer*. 2008;113(4):815–825.

37. Ishihara K, Yamagishi N, Hatayama T. Suppression of heat- and polyglutamine-induced cytotoxicity by nonsteroidal anti-inflammatory drugs. *Eur J Biochem*. 2004;271(22):4552–4558.

38. Yamanaka K, Takahashi N, Ooie T, Kaneda K, Yoshimatsu H, Saikawa T. Role of protein kinase C in geranylgeranylacetone-induced expression of heat-shock protein 72 and cardioprotection in the rat heart. *J Mol Cell Cardiol*. 2003;35(7):785–794.

39. Sidell N. Retinoic acid-induced growth inhibition and morphologic differentiation of human neuroblastoma cells *in vitro*. *J Natl Cancer Inst*. 1982;68(4):589–596.

40. Cheung YT, Lau WK, Yu MS, et al. Effects of all-*trans*-retinoic acid on human SH-SY5Y neuroblastoma as *in vitro* model in neurotoxicity research. *Neurotoxicology*. 2009;30(1):127–135.

41. Aggarwal BB, Ichikawa H. Molecular targets and anticancer potential of indole-3-carbinol and its derivatives. *Cell Cycle*. 2005;4(9): 1201–1215.

42. Rogan EG. The natural chemopreventive compound indole-3-carbinol: state of the science. *In Vivo*. 2006;20(2):221–228.

43. Chai Y, Koppenhafer SL, Bonini NM, Paulson HL. Analysis of the role of heat shock protein (Hsp) molecular chaperones in polyglutamine disease. *J Neurosci*. 1999;19(23):10338–10347.

44. Lee LC, Chen CM, Chen FL, et al. Altered expression of HSPA5, HSPA8 and PARK7 in spinocerebellar ataxia type 17 identified by 2-dimensional fluorescence difference in gel electrophoresis. *Clin Chim Acta*. 2009;400(1–2):56–62.

45. Chen CM, Lee LC, Soong BW, et al. SCA17 repeat expansion: mildly expanded CAG/CAA repeat alleles in neurological disorders and the functional implications. *Clin Chim Acta*. 2010;411(5–6):375–380.

46. Fujimoto M, Takaki E, Hayashi T, et al. Active HSF1 significantly suppresses polyglutamine aggregate formation in cellular and mouse models. *J Biol Chem*. 2005;280(41):34908–34916.

47. Fujikake N, Nagai Y, Popiel HA, Okamoto Y, Yamaguchi M, Toda T. Heat shock transcription factor 1-activating compounds suppress polyglutamine-induced neurodegeneration through induction of multiple molecular chaperones. *J Biol Chem*. 2008;283(38):26188–26197.

48. Choi Y, Kim Y, Park S, Lee KW, Park T. Indole-3-carbinol prevents diet-induced obesity through modulation of multiple genes related to adipogenesis, thermogenesis or inflammation in the visceral adipose tissue of mice. *J Nutr Biochem*. 2012;23(12):1732–1739.

49. Wu TY, Saw CL, Khor TO, Pung D, Boyanapalli SS, Kong AN. In vivo pharmacodynamics of indole-3-carbinol in the inhibition of prostate cancer in transgenic adenocarcinoma of mouse prostate (TRAMP) mice: involvement of Nrf2 and cell cycle/apoptosis signaling pathways. *Mol Carcinog*. 2012;51(10):761–770.

50. Crotti A, Benner C, Kerman BE, et al. Mutant Huntingtin promotes autonomous microglia activation via myeloid lineage-determining factors. *Nat Neurosci*. 2014;17(4):513–521.

51. Johri A, Beal MF. Antioxidants in Huntington's disease. *Biochim Biophys Acta*. 2012;1822(5):664–674.

52. Humphrey GR, Kuethe JT. Practical methodologies for the synthesis of indoles. *Chem Rev*. 2006;106(7):2875–2911.

53. Cacchi S, Fabrizi G. Update 1 of: Synthesis and functionalization of indoles through palladium-catalyzed reactions. *Chem Rev*. 2011;111(5): PR215–PR283.